2011 9th IEEE International Conference on
Control and Automation (ICCA)
Santiago, Chile, December 19-21, 2011

Improved Servomechanism Control Design - Dynamically Damped Case

Aurélio T. Salton, Zhiyong Chen and Minyue Fu

Abstract— **Time optimal control (TOC) for servomechanism is not a practical controller due to the chattering phenomenon that occurs on the presence of noise and model uncertainty. Maybe the most popular attempt to transform this controller in a practical one comes from the so called Proximate Time Optimal Servomechanism (PTOS). This approach starts with a near time optimal controller and then switches to a linear controller when the system output approaches the target. While the chattering phenomenon is avoided, this comes at an expense in performance generated by the so called "acceleration discount factor". This paper will present a controller that makes use of dynamic damping in order to push the acceleration discount factor arbitrarily close to one, thus practically eliminating the conservatism present in the PTOS. Experimental results support the proposed design.**

I. Introduction

In many automatic control systems, the most important performance requirement concerns minimum-time output response. However, it is well known that Time Optimal Control (TOC) [1] is not a practical controller inasmuch as both a perfect knowledge of the system and noise free measurements are necessary in order to avoid the chattering phenomenon [2]. Many different strategies have been proposed in order to overcome this problem, some of which take direct account of the controller saturation limits, such as the famous Proximate Time Optimal Servomechanism (PTOS) [3], and others which adopt a more "linear" approach, such as the smart Composite Nonlinear Feedback (CNF) [4]. The main objective of this paper is to propose the integration of the aforementioned techniques, so that, the merits of one are used to compensate the defects of the other.

Workman's PTOS is an important adaptation of the original TOC which takes into account the saturation levels of the input, but only makes use of them when it is practical to do so. As the system approaches the reference point, where chattering would normally occur, the PTOS switches to a linear controller and, therefore, elegantly deals with measurement noises and plant uncertainties. The chattering phenomenon does not occur with this strategy, it is famously easy to tune the controller, and a single set of parameters perform well for a wide range of set point changes. However, due to the fact that a linear controller is used when the system approaches the set point, necessarily some conservatism must be added such that a nonovershooting response is achieved. This is done via the so called "acceleration discount factor" which reduces the speed of the system to levels that can be dealt with by the linear controller.

On the other hand, Lin *et al.* [4] proposed a nonlinear technique for the improvement of linear systems performance. The controller is divided in two parts, a linear gain designed such that the system has a small damping for fast rise time, and a nonlinear function designed to add damping to the system as it approaches the reference point, thus avoiding unacceptable levels of overshoot. The best of two worlds is achieved by such method: a fast rise time with no or limited overshoot. This strategy was further developed by Chen *et al.* [5] and came to be known as Composite Nonlinear Feedback (CNF). As mentioned before, the CNF design itself does not explicitly take into account the saturation levels of the actuators. This makes the controller tuning somehow tedious once different parameters must be used for different ranges of actuation. However, an attempt to address this matter was made in [6] where an automatic tuning method is proposed.

By combining both controllers a significant improvement in performance may be achieved. The general framework of the PTOS is maintained, but, instead of switching the controller to the linear PD gain as the system approaches the reference point, this paper proposes a controller that switches to a simple form of CNF. In this way, damping may be added to the system resulting in a more aggressive usage of the PTOS, where the acceleration discount factor may be pushed to its limit, arbitrarily close to one. Furthermore, because the CNF is only employed in a very small range (when the system is close enough to the reference point), the tuning problems associated with such controller are minimized. The proposed design presents a considerable improvement in performance, is as easy to be tuned as the original PTOS, and with a single set of parameters performs well for a very wide range of set point variations.

The rest of the paper is organized as follows. Section 2 will present the model of interest along with a form of disturbance observer that is used to fit a larger class of systems to the rigid body dynamics model. Section 3 will present the proposed control design. Section 4 will expose experimental results and concluding remarks will be given in Section 5.

This work was partly supported by the Australian Research Councils Center of Excellence for Complex Dynamic Systems and Control (CDSC).

The authors are with the School of Electrical Engineering and Computer Science, The University of Newcastle, Callaghan, NSW 2308, Australia. aurelio.salton@uon.edu.au, {zhiyong.chen, minyue.fu}@newcastle.edu.au

M. Fu is also with the Department of Control Science and Engineering, Zhejiang University, China.

Z. Chen is also with the State Key Laboratory of Digital Manufacturing Equipment and Technology, Huazhong University of Science and Technology.

978-1-4577-1476-4/11/$26.00 ©2011 IEEE

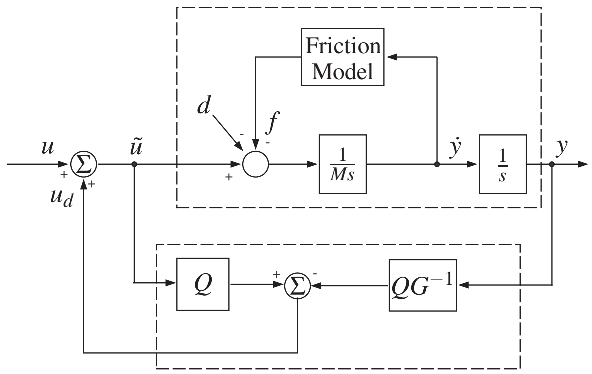

Fig. 1. The model-based friction compensator.

II. Dynamic Model and Friction Compensator

The system in hand is comprised of a body of mass M subject to some friction f and disturbance d,

$$M\ddot{y} = \tilde{u} - f - d.$$

Once friction and disturbances are undesirable phenomena that exert adverse effects on the tracking performance, the model-based friction compensator of Fig. 1 will be employed. This is a mature compensator that has been successfully implemented in previous applications [7]; [8] and [9]. In the structure given at the figure, G is the desired dynamics of the system:

$$G = \tfrac{1}{Ms^2}, \tag{1}$$

and Q is any filter that can be approximated as one within the bandwidth of interest ($Q \approx 1$). In this way, the input-output relation in Fig. 1 becomes:

$$y = \tfrac{u-(1-Q)(d+f)}{Ms^2} \approx \tfrac{1}{Ms^2}u, \tag{2}$$

and the system is fully described by the rigid body equations of motion given by:

$$\begin{aligned} \dot{x}_1 &= x_2 \\ \dot{x}_2 &= b\,\mathrm{sat}(u) \\ y &= x_1 \end{aligned} \tag{3}$$

where x_1 and x_2 refer to the position and velocity, $b := 1/M$ and "sat" is the saturation function defined as:

$$\mathrm{sat}(z) = \begin{cases} \bar{u}, & z > \bar{u} \\ z, & |z| < \bar{u} \\ -\bar{u}, & z < -\bar{u} \end{cases} \tag{4}$$

with $\bar{u}$ the saturation level of the control input.

It is the system described by (3) that will be considered in the remainder of this paper.

III. Control Design

The original Proximate Time Optimal Servomechanism (PTOS) is an adaptation from the time optimal, or bang-bang, controller. It also uses the maximal acceleration the system is able to deliver, but only when it is practical to do so. As the system approaches the reference point the PTOS switches to a linear controller in order to avoid chattering and achieve asymptotical stability. This linear controller, however, is unable to avoid the overshoot if the system approaches the reference with a large speed. In order to overcome this problem the so called acceleration discount factor ($0 < \alpha < 1$) was introduced in the nonlinear function that emulates the time optimal controller. The result is a controller that achieves acceptable levels of overshoot, but that is somehow conservative.

The PTOS as presented by [3] is given by

$$u = k_2(-f_{ptos}(e) - v), \tag{5}$$

with,

$$f_{ptos}(e) = \begin{cases} (k_1/k_2)e, & \text{for } |e| \le y_l, \\ \mathrm{sgn}(e)(\sqrt{2b\alpha\bar{u}|e|} - \bar{u}/k_2), & \text{for } |e| > y_l. \end{cases} \tag{6}$$

Where we have defined $e := x_1 - y_r$ and $v := x_2$. Furthermore, in order to guarantee the continuity of the controller during the switching, the following conditions must be satisfied:

$$y_l = \frac{\bar{u}}{k_1}, \;\; k_2 = \sqrt{\frac{2k_1}{b\alpha}}. \tag{7}$$

Notice there are two free parameters in the design of the PTOS, namely k_1 and α. Both these parameters should be as large as possible, but, as mentioned before, the design must be somehow conservative in the choice of α in order to avoid unacceptable levels of overshoot. This is due to the relation between α and k_2. Recall that the PD controller gain for rigid body systems may be parameterized as a function of the undamped natural frequency ω_n and damping ratio ζ:

$$K = \frac{1}{b}[4\pi^2\omega_n^2 \;\; 4\pi\omega_n\zeta]. \tag{8}$$

Together with the second equation in (7), we find that ζ is directly dependent in the choice of α in the following way

$$\zeta = \sqrt{\frac{1}{2\alpha}} \tag{9}$$

It is now clear that if we try to push $\alpha \to 1$ we will necessarily be pushing the damping ratio to $\zeta \to 0.707$ and, unfortunately, an unacceptable level of overshoot will occur. Therefore, it is logical to attempt to use a form of dynamic damping in order to solve the overshooting problem while achieving $\alpha \to 1$. In this way we may satisfy the continuity constraints given by (7), achieve an improvement in performance by making an aggressive choice of α and still avoid undesired levels of overshoot. Such controller is the main contribution of this paper and is presented in the next theorem.

Theorem 3.1: Consider system (3) with

$$u = k_2(-f(e) - \rho(e)v), \tag{10}$$

where,

$$f(e) = \begin{cases} (k_1/k_2)e, & \text{for } |e| \le y_l, \\ \mathrm{sgn}(e)(\sqrt{2b\alpha\bar{u}|e|} - \bar{u}/k_2), & \text{for } |e| > y_l, \end{cases} \tag{11}$$

and

$$\rho(e) = \begin{cases} 1 + \beta(|e| - y_l)^2, & |e| \le y_l, \\ 1, & |e| > y_l. \end{cases} \tag{12}$$

With

$$k_1 > 0,\ k_2 = \sqrt{\frac{2k_1}{b\alpha}},\ y_l = \frac{\bar{u}}{k_1} \tag{13}$$

and

$$0 < \alpha < 1,\ (\alpha^{-1} - 1)/(4y_l^2) > \beta \ge 0. \tag{14}$$

Then, the closed-loop system is globally asymptotically stable in the sense that $\lim_{t\to\infty} x(t) = 0$ for any $x(0) \in \mathbb{R}^2$. ∎

Proof: Without loss of generality, we assume $y_r = 0$ and the problem reduces to a stabilization problem of the equilibrium point $x := [x_1, x_2]^\mathsf{T} = 0$. We proceed by noticing that the control law (10) may be described as:

$$u = -h_1(x_1) - h_2(x_1)x_2, \tag{15}$$

where $h_1(\cdot)$ and $h_2(\cdot)$ are piecewise continuously differentiable functions, with $h_1(0) = 0$, given by:

$$\begin{aligned} h_1(x_1) &:= k_2 f(x_1), \\ h_2(x_1) &:= k_2 \rho(x_1). \end{aligned} \tag{16}$$

The proof will be divided in three parts showing that: *(i)* Given an unsaturated region $\mathbb{U}$ defined by,

$$\mathbb{U} = \{(x_1,\ x_2) \in \mathbb{R}^2 \mid |-h_1(x_1) - h_2(x_1)x_2| \le \bar{u}\},$$

any trajectory starting outside $\mathbb{U}$ enters $\mathbb{U}$ in finite time; *(ii)* Any trajectory in $\mathbb{U}$ remains there indefinitely; *(iii)* Once in $\mathbb{U}$ the trajectory converges to the equilibrium point, i.e., $\lim_{t\to\infty} x(t) = 0$.

(i) Suppose a given initial condition $(x_1(0),\ x_2(0))$ belongs to the region outside $\mathbb{U}$ where $u(0) > \bar{u}$, that is,

$$u(0) = -h_1(x_1(0)) - h_2(x_1(0))x_2(0) > \bar{u}.$$

It must be shown that for a finite time $T > 0$, the input will be such that $u(T) = \bar{u}$. From the system equations (3), the evolution of the system will be:

$$\begin{aligned} x_2(t) &= b\bar{u}t + x_2(0) > 0 \\ x_1(t) &= b\bar{u}t^2/2 + x_2(0)t + x_1(0) > 0 \end{aligned}$$

for a sufficiently large t. Since[1] $h_1'(x_1) > 0$ and $h_2(x_1) > 0$, we have $h_2(x_1(t))x_2(t) > 0$ and,

$$\begin{aligned} u(t) &= -h_1(x_1(t)) - h_2(x_1(t))x_2(t) \\ &< -h_1(b\bar{u}t^2/2 + x_2(0)t + x_1(0)). \end{aligned}$$

Therefore $u(t)$ satisfies $\lim_{t\to\infty} u(t) = -\infty$, and, due to the continuity of $h_i(\cdot)$, it must be that $u(t)$ takes all the values in the interval $[u(0),\ -\infty)$. Which implies that for a finite time $T > 0$, $u(T) = \bar{u}$, i.e., the system enters $\mathbb{U}$. By symmetry, the same is true for trajectories satisfying $u(0) < -\bar{u}$.

(ii) In order to prove that any trajectory starting in $\mathbb{U}$ will remain there indefinitely, let T denote the time when the trajectories are at the boundary of $\mathbb{U}$, that is $|u(T)| = \bar{u}$. These trajectories will stay in $\mathbb{U}$ if,

$$u(T)\dot{u}(T) < 0, \tag{17}$$

where $\dot{u} = -(h_1'(x_1)\dot{x}_1 + h_2(x_1)\dot{x}_2 + h_2'(x_1)\dot{x}_1 x_2)$ is the change rate of u, because either $u(T) = \bar{u}$ and $\dot{u} < 0$, or $u(T) = -\bar{u}$ and $\dot{u} > 0$. We consider the case when $u(T) = \bar{u}$, then,

$$\begin{aligned} \dot{u} &= -(h_1'x_2 + h_2 b\bar{u} + h_2'x_2^2) \\ &= h_1'(\frac{\bar{u} + h_1}{h_2}) - h_2 b\bar{u} - h_2'(\frac{\bar{u} + h_1}{h_2})^2 \\ &= \frac{h_1'h_1}{h_2} + \frac{h_1'\bar{u}}{h_2} - h_2 b\bar{u} - h_2'(\frac{\bar{u} + h_1}{h_2})^2 < 0 \end{aligned} \tag{18}$$

is guaranteed by (14). Next, we consider the case when $u(T) = -\bar{u}$, then, a similar calculation shows

$$\dot{u} = \frac{h_1'h_1}{h_2} - \frac{h_1'\bar{u}}{h_2} + h_2 b\bar{u} - h_2'(\frac{\bar{u} - h_1}{h_2})^2 > 0 \tag{19}$$

is also guaranteed by (14).

(iii) We may now proceed to the stability proof of the system when inside the region $\mathbb{U}$ and neglect the effects of saturation. To do so, let us take the following as a Lyapunov function candidate

$$V(x) = \int_0^{x_1} h_1(y)dy + \frac{x_2^2}{2b}. \tag{20}$$

which is positive definite and radially unbounded.

Along the trajectory of the closed-loop system inside the region $\mathbb{U}$, we have

$$\begin{aligned} \dot{V}(x) &= h_1(x_1)x_2 - x_2[h_1(x_1) + h_2(x_1)x_2] \\ &= -h_2(x_1)x_2^2 \le 0. \end{aligned}$$

It remains to show that $\dot{V}(x) = 0$ only at the origin

$$\dot{V}(x) = 0 \Rightarrow h_2(x_1)x_2^2 = 0 \Rightarrow x_2 = 0.$$

Which in turn implies that

$$x_2(t) = 0 \Rightarrow \dot{x}_2(t) = 0 \Rightarrow h_1(x_1(t)) = 0 \Rightarrow x_1(t) = 0.$$

We may now claim LaSalle's invariance principle and assert that $\lim_{t\to\infty} x(t) = 0$. This completes the proof. □

[1] We define $h_i'(x_1) := dh_i(x_1)/dx_1$ as the derivative of h_i and drop the dependency of the functions on x_1 for ease of notation, if it does not cause any confusion.

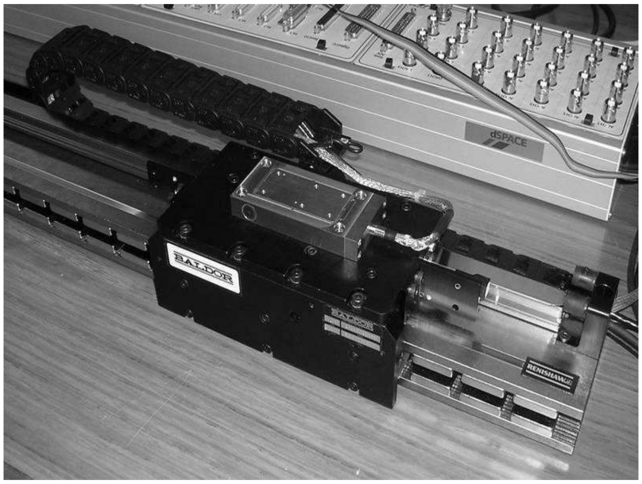

Fig. 2. Experimental set up of the electromagnetic motor.

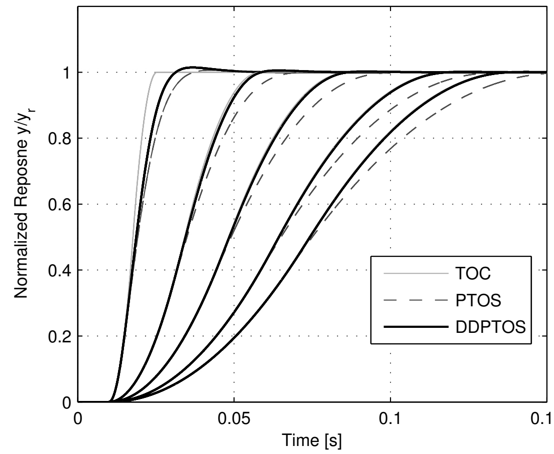

Fig. 3. Normalized simulated responses (y/y_r) for steps of 1, 10, 25, 50 and 70 mm for the three comparative controllers.

Notice that the control law (10) is very similar to that of (5), the only difference coming from the inclusion of the term $\rho(e)$. If fact, by choosing $\rho(e) = 1$ the proposed controller becomes the traditional PTOS. This nonlinear term, however, provides the system with dynamic damping when it enters the region $|e| \leq y_l$, which, in turn, allows us to be extremely aggressive when $|e| > y_l$, pushing $\alpha \to 1$ and eliminating the conservatism present in the original PTOS. Since now α is only necessary for stability issues and may be arbitrarily close to one, e.g., $\alpha = 0.99$, there are still only two free parameters to be tuned, namely k_1 and β, which means that the tuning process of the proposed controller is as easy and as straightforward as that of the PTOS.

IV. Results

In this section we will show simulated and experimental results of the proposed control design. In order to compare its performance, we will also simulate and implement the traditional PTOS, and compare both controllers to the simulated time optimal controller. The system in hand is the linear motor depicted in Fig. 2 whose parameters are $b = 1.7 \times 10^4$ and $\bar{u} = 1$. The time optimal control law is given by

$$u_{to}(t) \quad = \quad \mathrm{sgn}(\sqrt{2b\bar{u}|e|} - v). \qquad (21)$$

and the parameters of the prosed design and of the original PTOS are as described in Table 1.

Figure 3 presents the simulated normalized responses to step references of 1, 10, 25, 50 and 70 mm. The thin gray line is the TOC, the dashed line is the original PTOS and the dark line is the proposed Dynamically Damped Proximate Time Optimal Servomechanism (DDPTOS). One can see that the prosed design presents a clear improvement over the traditional controller and is much closer to the theoretical limits given by the TOC. This is even clearer in Fig. 4, where we have zoomed in the 70 mm step. Notice how the proposed design practically matches the TOC. Also notice the bottom plot in the figure where the similarity between the inputs of the proposed controller and the TOC are evident.

TABLE I
CONTROLLERS' PARAMETERS

Parameter	Traditional	Proposed
k_1	2.09	2.09
k_2	0.019	0.016
α	0.7	0.99
β	-	0.02

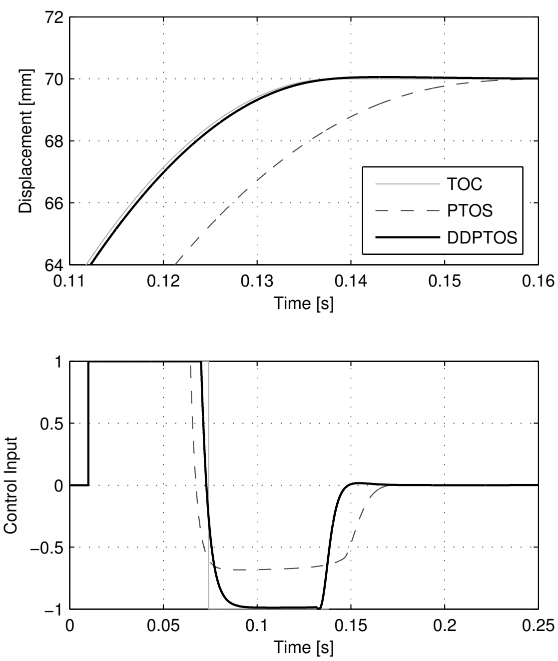

Fig. 4. Simulated response of TOC, PTOS and DDPTOS for a 70 mm step reference.

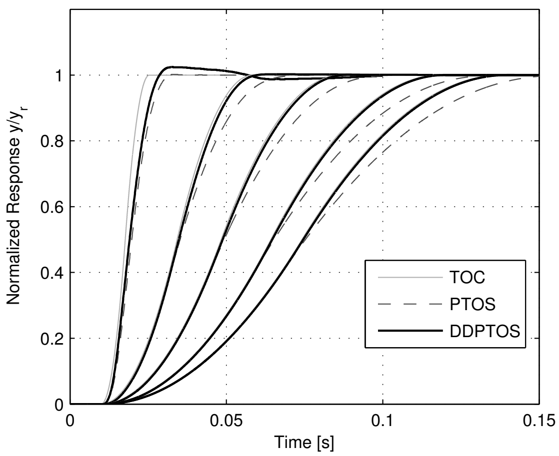

Fig. 5. Normalized plant responses (y/y_r) for steps of 1, 10, 25, 50 and 70 mm for the two compared controllers along with simulated TOC responses.

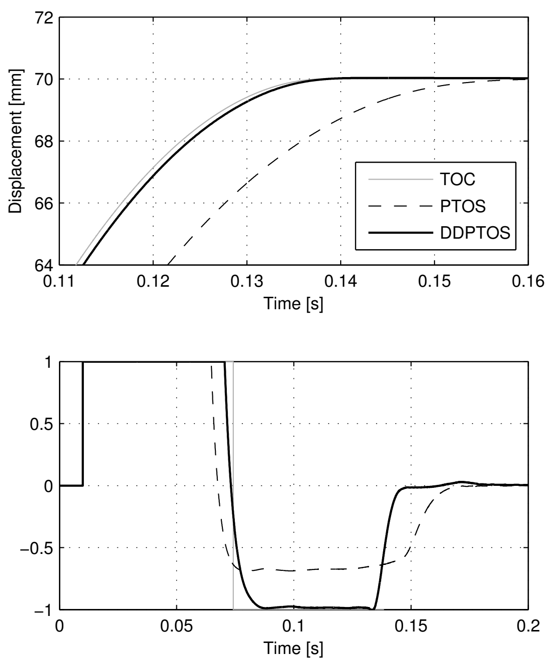

Fig. 6. Simulated response of the TOC and plant responses of PTOS and DDPTOS for a 70 mm step reference.

The experimental results seen in Figures 5 and 6 support the performance improvement seen in the simulation responses. It is clear that a significant improvement is achieved by the proposed design. In fact, the proposed controller performance is indeed comparable to that of the simulated TOC.

V. Conclusion

This paper proposed a form of active damping in order to improve the performance of the well known Proximate Time Optimal Servomechanism (PTOS). The proposed design is able to practically eliminate the conservatism present in the original PTOS by pushing the so called "acceleration discount factor" arbitrarily close to one. The main contribution of the paper is to achieve a performance comparable to that of the theoretical limits given by Time Optimal Control while retaining acceptable levels of overshoot. Experimental results give support to the proposed control design.

References

[1] Bryson, A. E. and Ho, Y. C., *Applied Optimal Control.* New York: Hemisphere, 1975.

[2] Khalil, H. K., *Nonlinear Systems,* 3rd ed. Upper Saddle river, NJ: Prentice Hall, 2002.

[3] M.L. Workman, R.L. Kosut, and G.F. Franklin, "Adaptive proximate time-optimal servomechanisms- Continuous time case," *6th American Control Conference*, pp. 589-594, Minneapolis, MN, 1987.

[4] Z. Lin, M. Pachter, and S. Banda, "Toward improvement of tracking performance-nonlinear feedback for linear systems," *Int. Journal of Control*, vol. 70, pp. 1-11, 1998.

[5] B. M. Chen, T. H. Lee, K. Peng, and V. Venkataramanan, "Composite nonlinear feedback control for linear systems with input saturation: theory and an application," *IEEE Trans. Automatic Control*, vol. 48, no. 3, pp. 427-439, Mar. 2003.

[6] W. Lan, C.K. Thum and B.M. Chen, "A Hard-Disk-Drive Servo System Design Using Composite Nonlinear-Feedback Control With Optimal Nonlinear Gain Tuning Methods," *IEEE Trans. Inddustrial Electronics*, vol.57, no.5, pp.1735-1745, May 2010

[7] J. Zheng, A.T. Salton and M. Fu, "A Novel Rotary Dual-Stage Actuator Positioner," *In Proceedings of the 48th IEE Conference on Decision and Control*, pages 5426-5431, Dec. 2009.

[8] A.T. Salton, Z. Chen, J. Zheng and M. Fu, "Preview Control of Dual-Stage Actuator Systems for Super Fast Transition Time," *IEEE/ASME Trans. Mech. (99),* pages1-6 [Online]. Avilable: http://ieeexplore.ieee.org, DOI: 10.1109/TMECH.2010.2053851.

[9] A.T. Salton, Z. Chen and M. Fu, "Improved Control Design Methods for Proximate Time Optimal Servomechanisms," *IEEE/ASME Trans. Mechatronics,* to appear, 2010.